ISSN 1063-7834, Physics of the Solid State, 2016, Vol. 58, No. 3, pp. 462–468. © Pleiades Publishing, Ltd., 2016.
Original Russian Text © A.B. Gordienko, A.V. Kosobutsky, 2016, published in Fizika Tverdogo Tela, 2016, Vol. 58, No. 3, pp. 451–457.

SEMICONDUCTORS

Analysis of the Electronic Structure of Crystals through Band Structure Unfolding

A. B. Gordienko[a, *] and A. V. Kosobutsky[a,b]

[a] *Kemerovo State University, ul. Voroshilova 17, Kemerovo, 650056 Russia*
[b] *National Research Tomsk State University, pr. Lenina 36, Tomsk, 634050 Russia*
**e-mail: gordi@kemsu.ru*

Received July 14, 2015

Abstract—In this work, we consider an alternative implementation of the band structure unfolding method within the framework of the density functional theory, which combines the advantages of the basis of localized functions and plane waves. This approach has been used to analyze the electronic structure of the ordered $CuCl_xBr_{1-x}$ copper halide alloys and F^0 center in MgO that enables us to reveal qualitatively the features remaining hidden when using the standard supercell method, because of the complex band structure of systems with defects.

DOI: 10.1134/S1063783416030124

1. INTRODUCTION

Theoretical methods of characterization of the electronic structure in crystalline solids, based on spatial periodicity, are currently applied for simulation of not only perfect crystals, but systems with irregular repeatability of the structural elements, such as point defects, interfaces, superlattices, alloys, and others. In this case, the required translation symmetry is artificially maintained due to the description of the structure via the unit cell expansion in the main crystal [1] that results in the calculations using supercells. As a result, the electron spectrum becomes strongly complicated and acquires multiband behavior that impedes its analysis, particularly from the point of view of the changes caused by the perturbations that violate the periodicity of the main crystal. On the other hand, since the perturbations are generally subjected to localized behavior, the complexity of the electronic spectrum is mainly due to band structure folding, which means one has the ability to study the electronic structure of a complex crystal on the basis of the translation symmetry of the main crystal. This approach is called band structure unfolding and was earlier considered in [2–6]. Actually, there is great interest in theoretical investigations of band unfolding when analyzing the properties of solid solutions [7–10], surface states [11–13] and point defects in nanostructures [14, 15].

The effective band structure obtained via unfolding allows visualizing the effect of the translation symmetry violation on the dispersion dependence $E(\mathbf{k})$ and assumes direct comparison with the angle-resolved photoelectron spectroscopy data. The methods for practical implementation of this approach proposed in the literature are different in the type of the basis that is used in the calculations of the electronic structure of crystals. So, the plane wave basis is used in [3, 8–10, 13, 15], while the basis of functions localized at the atoms is applied in [4–7, 11, 12, 14]. In this work, the band unfolding is implemented for the basis of the localized functions in the form of pseudoatomic orbitals (PAOs) [16–18]. The method, the results of the test calculations for perfect silicon crystals, as well as an analysis of the electronic structure of the ordered $CuCl_xBr_{1-x}$ copper halide alloys and a vacancy defect (F^0 center) in MgO, are presented below.

2. BAND UNFOLDING FOR PAO BASIS

In the discussion of the band unfolding method applied to the lattices with the primitive cell (PC) and extended cell (EC), it is convenient to use the designations from [8, 12]. A relationship between the translation vectors of a PC-lattice ($\mathbf{a}_i$, $i = 1, 2, 3$) and EC-lattice ($\mathbf{A}_i$) can be presented, as follows:

$$\mathbf{A}_i = \sum_{j=1}^{3} M_{ij}\mathbf{a}_i, \qquad (1)$$

where M_{ij} is the nonsingular matrix with integer elements, and the magnitude $\nu = \det M$ equals the EC-to-PC volume ratio and the number of vectors $\mathbf{r}_i$, $i = 1,\ldots, N$, which can be used for completing the EC area by

translation of PC [12]. By analogue, we can write for the main vectors of the reciprocal PC- and EC-lattices

$$\mathbf{B}_i = \sum_{j=1}^{3} (M^T)^{-1}_{ij} \mathbf{b}_j. \quad (2)$$

As follows from (2), the points of PC- and EC- Brillouin zones are related to each other by an expression

$$\mathbf{k} = \mathbf{K} + \mathbf{G}_\mathbf{K}, \quad \mathbf{G}_\mathbf{K} = m_1\mathbf{B}_1 + m_2\mathbf{B}_2 + m_3\mathbf{B}_3. \quad (3)$$

The wave vector value characterizes the properties of the translation symmetry of $\psi_{n\mathbf{k}}$ or $\psi_{N\mathbf{K}}$ states. As an example, we have for a PC-lattice

$$T(\mathbf{a})\psi_{n\mathbf{k}} = e^{i\mathbf{k}\mathbf{a}}\psi_{n\mathbf{k}}, \quad (4)$$

where $T(\mathbf{a})$ is the translation operator to a vector of the EC-lattice ($\mathbf{a} = n_1\mathbf{a}_1 + n_2\mathbf{a}_2 + n_3\mathbf{a}_3$). Therefore, if the translation symmetry of a PC-lattice is preserved after any expansion, expression (4) will also be valid for $\psi_{N\mathbf{K}}$ states, and the relationship (3) will describe the folding of $E_{n\mathbf{k}}$ bands of a PC-lattice into the Brillouin zone of a EC-lattice ($E_{N\mathbf{K}}$), accompanied by the additional degenerations of $E_{N\mathbf{K}}$ bands in the points at the Brillouin zone boundaries of the EC-lattice. If the translation symmetry of the PC-lattice built-in a EC-lattice is broken, expression (4) for $\psi_{N\mathbf{K}}$ states is not valid. The $\psi_{N\mathbf{K}}$ states can, however, include a part which obeys this expression and can be obtained according to the general idea of the band unfolding method via the projection onto the states with the translation symmetry of $\mathbf{k}$-point. For the purposes of this work, it is more convenient to use the following expression for a $W_{\mathbf{K}N}(\mathbf{G}_\mathbf{K})$ weight [12]:

$$W_{\mathbf{K}N}(\mathbf{G}_\mathbf{K}) = \frac{1}{\nu}\sum_{j=1}^{\nu} \langle\psi_{N\mathbf{K}}|T(\mathbf{r}_j)|\psi_{N\mathbf{K}}\rangle e^{-i(\mathbf{K}+\mathbf{G}_\mathbf{K}))\mathbf{r}_j}, \quad (5)$$
$$0 \le W_{\mathbf{K}N} \le 1.$$

In turn, the $E_{N\mathbf{K}}$ band structure unfolded into the Brillouin zone of the PC-lattice can be presented using the spectral function:

$$A(\mathbf{k}, E) = \sum_N W_{\mathbf{K}N}(\mathbf{G}_\mathbf{K})\delta(E - E_{N\mathbf{K}}). \quad (6)$$

Expression (5) is general, but the method for calculating $A(\mathbf{k}, E)$ depends on the representation of $\psi_{N\mathbf{K}}$. For the basis of the localized function, we have

$$\psi_{N\mathbf{K}}(\mathbf{r}) = \sum_\mu C_\mu^{N\mathbf{K}}\Phi_{\mu\mathbf{K}}(\mathbf{r}). \quad (7)$$

Here, $\Phi_{\mu\mathbf{K}}(\mathbf{r})$ are the basis Bloch functions constructed as the lattice sums of the localized $\varphi_i(\mathbf{r})$ functions centered at the atoms of the crystal at the positions $\boldsymbol{\tau}_\mu$:

$$\Phi_{\mu\mathbf{K}}(\mathbf{r}) = \frac{1}{\sqrt{\Omega}}\sum_\mathbf{A} e^{i\mathbf{K}(\mathbf{A}+\boldsymbol{\tau}_\mu)}\varphi_\mu(\mathbf{r} - \mathbf{A} - \boldsymbol{\tau}_\mu), \quad (8)$$

where Ω is the crystal volume. In this work, the pseudoatomic orbitals are used as $\varphi_i(\mathbf{r})$ [16–18]. For calculation of the matrix Hamiltonian elements and overlap integrals with nonorthogonal functions (8), it is convenient to use their representation as the Fourier series in the reciprocal lattice:

$$\Phi_{\mu\mathbf{K}}(\mathbf{r}) = \frac{1}{\sqrt{\Omega}}\sum_\mathbf{G} \tilde{\Phi}_{\mu\mathbf{K}}(\mathbf{G})e^{i(\mathbf{K}+\mathbf{G})\mathbf{r}}, \quad (9)$$

$$\tilde{\Phi}_{\mu\mathbf{K}}(\mathbf{G}) = \frac{1}{\sqrt{\Omega}}\sum_{(\Omega)} \Phi_{\mu\mathbf{K}}(\mathbf{r})e^{-i(\mathbf{K}+\mathbf{G})\mathbf{r}}d\mathbf{r}. \quad (10)$$

Substituting (9) in (7) and then in (5) and implementing the subsequent simple transformations, one can obtain the expression for the state weights in the form:

$$W_{\mathbf{K}N}(\mathbf{G}_\mathbf{K}) = \frac{1}{\nu}\sum_{j=1}^{\nu} e^{-i\mathbf{G}_\mathbf{k}\mathbf{r}_j}\sum_\mathbf{G}|\tilde{C}_\mathbf{G}^{N\mathbf{K}}|^2 e^{i\mathbf{G}\mathbf{r}_j}, \quad (11)$$

where

$$\tilde{C}_\mathbf{G}^{N\mathbf{K}} = \sum_\mu C_\mu^{N\mathbf{K}}\tilde{\Phi}_{\mu\mathbf{K}}(\mathbf{G}). \quad (12)$$

Expressions (11) and (12) were used for further calculations. It is worth mentioning that Eq. (11) by analogue with the formulas derived in [8, 13] for the plane wave basis indicates that the band unfolding method is, in fact, the Fourier filtering option applied to the states that are described by $\psi_{N\mathbf{K}}$ functions.

3. CALCULATION PARAMETERS AND CRYSTAL STRUCTURES

The electronic structure was calculated using the density functional theory (DFT) in the local approximation to describe the exchange effects and electronic correlations (LDA) [19, 20], as well as by means of the method of special points [21] to evaluate the electronic density. To describe the electron–ion interaction, the ab initio separable HGH-pseudopotentials were used [22]. All cases involved the basis of localized pseudoatomic Si(*ss*, *pp*, *dd*), Cu(*s*, *d*), Cl(*ss*, *pp*, *dd*), Br(*ss*, *pp*, *dd*), Mg(*s*, *p*, *d*), and O(*s*, *p*, *d*) SZ and DZ functions. In the decompositions of the basic functions (9) and (10), plane waves with energies to 16 Ry for silicon crystal, 169 Ry for $CuCl_xBr_{1-x}$, and 184 Ry in the case of MgO were taken into account.

The unfolding method was used for several cases of the construction of a EC-lattice. To verify implementation, a perfect silicon crystal was considered, subjected to a face-centered lattice with the basic translation vectors:

$$\mathbf{a}_1\left(0, \frac{a}{2}, \frac{a}{2}\right), \quad \mathbf{a}_2\left(\frac{a}{2}, 0, \frac{a}{2}\right), \quad \mathbf{a}_3\left(\frac{a}{2}, \frac{a}{2}, 0\right). \quad (13)$$

The band structure was calculated for a PC-lattice (13) and for two EC-lattices of silicon with the expanded

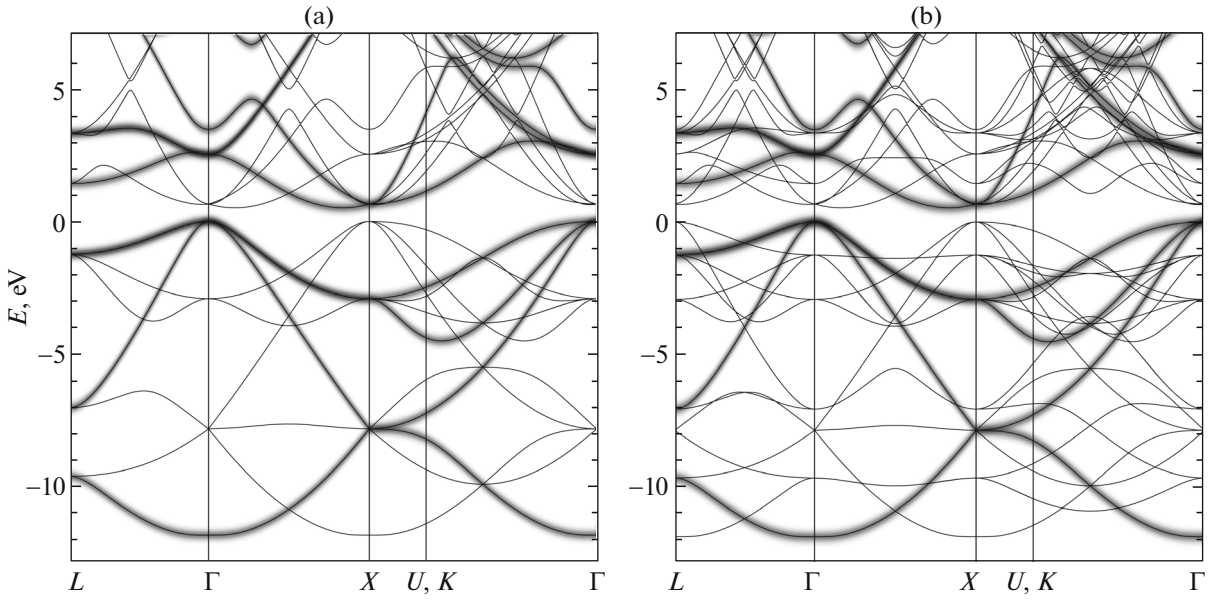

Fig. 1. Spectral function of silicon: (a) EC(4*x*) and (b) EC(8*x*). The dark color shows the bands with a maximum weight, and the thin lines correspond to the bands with a zero weight.

cell, for which the matrices M_{ij} in expression (1) were determined as

$$M^{[4x]} = \begin{pmatrix} -1 & 1 & 1 \\ 1 & -1 & 1 \\ 1 & 1 & -1 \end{pmatrix}, \quad M^{[8x]} = \begin{pmatrix} 2 & 0 & 0 \\ 0 & 2 & 0 \\ 0 & 0 & 2 \end{pmatrix} \qquad (14)$$

and correspond to four- and eight-fold PC expansion (13). Moreover, an EC(4*x*) lattice becomes cubic with eight atoms, whereas a EC(8*x*) one remains face-centered with 16 atoms. The electronic structure in copper halide alloys was investigated on the basis of the expanded cell constructed by simple expansion $M^{[8x]}$ of the unit cell (13) and by the subsequent substitution of the halogen atoms. To calculate the F^0-center in MgO, a 63-atom cell constructed by means of the symmetry expansion $M^{[8x]}$ of a cubic cell with $M^{[4x]}$ was used; i.e., $M^{[32x]} = M^{[4x]}M^{[8x]}$. Before calculating the electron spectra, the crystal structure was optimized via LDA. For $CuCl_xBr_{1-x}$ ($x = 0.25$, 0.50, and 0.75) compounds the optimized lattice parameters were taken from [23].

4. RESULTS AND DISCUSSION

Figure 1 displays the band structure of silicon for two EC-lattice configurations with a superposed spectral function calculated from the expression (6). As is seen, the profile $A(\mathbf{k}, E)$ in its maximum values completely recovers all typical features of the band structure of a PC-lattice that reveals the full reservation of the translation symmetry of a PC-lattice at simple expansions of the unit cell in perfect crystal.

As another example, the electronic structure of $CuCl_xBr_{1-x}$ alloy is considered, because it seems more attractive from the point of view of the band unfolding application. Copper halides are the direct-gap semiconductors with the bandgap width E_g of about 3 eV and are of interest in optoelectronics [24, 25]. We have previously demonstrated an ability to noticeably increase the accuracy of the calculations of E_g for these compounds by means of DFT, using the exchange potential TB09 [23]. In this work, we focus on the analysis of the spectral function, and all calculations were thus conducted using LDA.

Figures 2a and 2b display the band structures of CuBr and CuCl perfect crystals and are taken for the further analysis of the bands of alloys. Copper halides exhibit the qualitatively similar band structure with the valence band composed of three bands of allowed states which correspond to *s*- and *p*-states of halogen and *d*-states of copper in order of their increasing energy. Therefore, *p*–*d*-hybridization effects play important roles in the formation of two upper valence bands. We also mention that due to the different electronic structure of the halide atoms the energy levels of the valence *s*- and *p*-bands in CuCl are located lower than in CuBr by a value of 0.5 to 1.0 eV, while the free levels in CuCl with the predominant contribution of Cl *d*-orbitals are higher, and this difference is on the order of 1.0 eV at the Γ point.

Figures 2c–2e show the spectral functions of $CuCl_xBr_{1-x}$ alloys. As is seen, the translation symmetry of a PC-lattice is most preserved for alloy in the sense of (6), and its violations appear in the band ruptures typical for such representations of the electronic

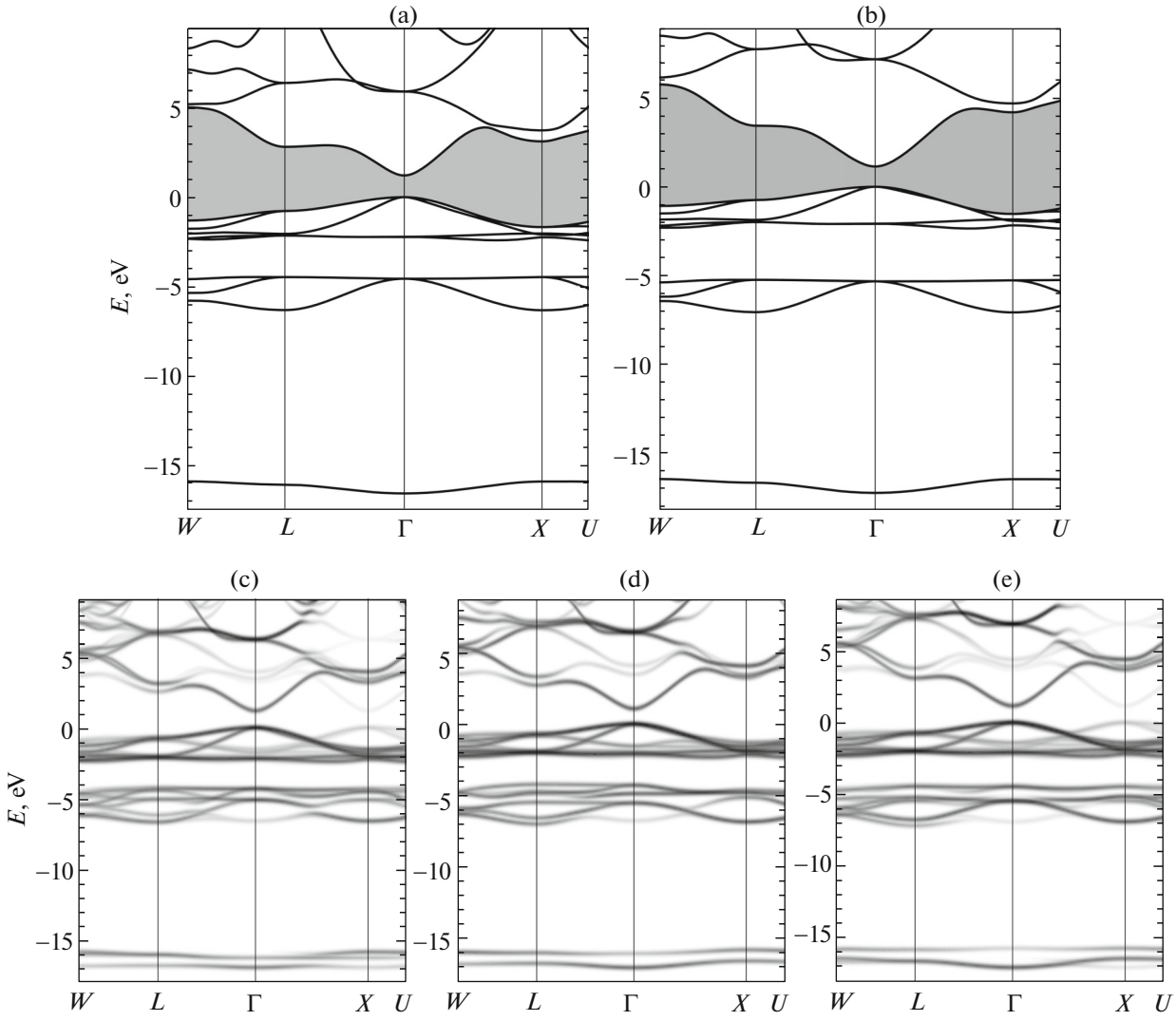

Fig. 2. Band structure for (a) CuBr and (b) CuCl (the band gap is marked with gray), and spectral function of $CuCl_xBr_{1-x}$ for $x = 0.25$ (c), 0.50 (d), and 0.75 (e).

structure. In common, the subsequent substitution of the band structure of CuBr with that of CuCl can be observed in the series $CuCl_xBr_{1-x}$, which is due to the increasing chlorine atom concentration. For the lowest *s*-bands of halogen the changes are the most obvious; where the long order for the chlorine atoms manifests itself at $x = 0.25$ and then at $x = 0.75$ the *s*-band of the chlorine atoms is almost completely recovered. Herewith, the behavior and location of *s*-bands allows arguing that there are no additional interactions of *s*-states of different halogen atoms during the formation of the solution or they are too small to induce the noticeable repulsion of levels.

The unfolded band structure is the most complex in the range of the valence *p*-states, where it looks like the superposition of valence *p*-bands in perfect crystals for all considered *x* values. The typical for the defect crystals a rupture of the p-bands with high contribution of the chlorine atom states is observed for alloy with $x = 0.25$ toward the direction Γ–X, but for $x = 0.5$ and 0.75 the dispersion dependences are smooth enough. It is seen that the compositional changes in the electronic structure in the *p*-bands of halides are qualitatively different from those considered above for *s*-states. This is due to the effect of the *p*–*d*-hybridization, which noticeably smooths the perturbations caused by variation in the atomic composition.

The unfolded band structure of $CuCl_xBr_{1-x}$ in the *d*-bands of copper accurately repeats all features of the *d*-bands in perfect copper crystals at all *x* values, which is due to the preservation of the initial translation symmetry in the cationic sublattice of alloys. In this case, the influence of the changes in the composition, how-

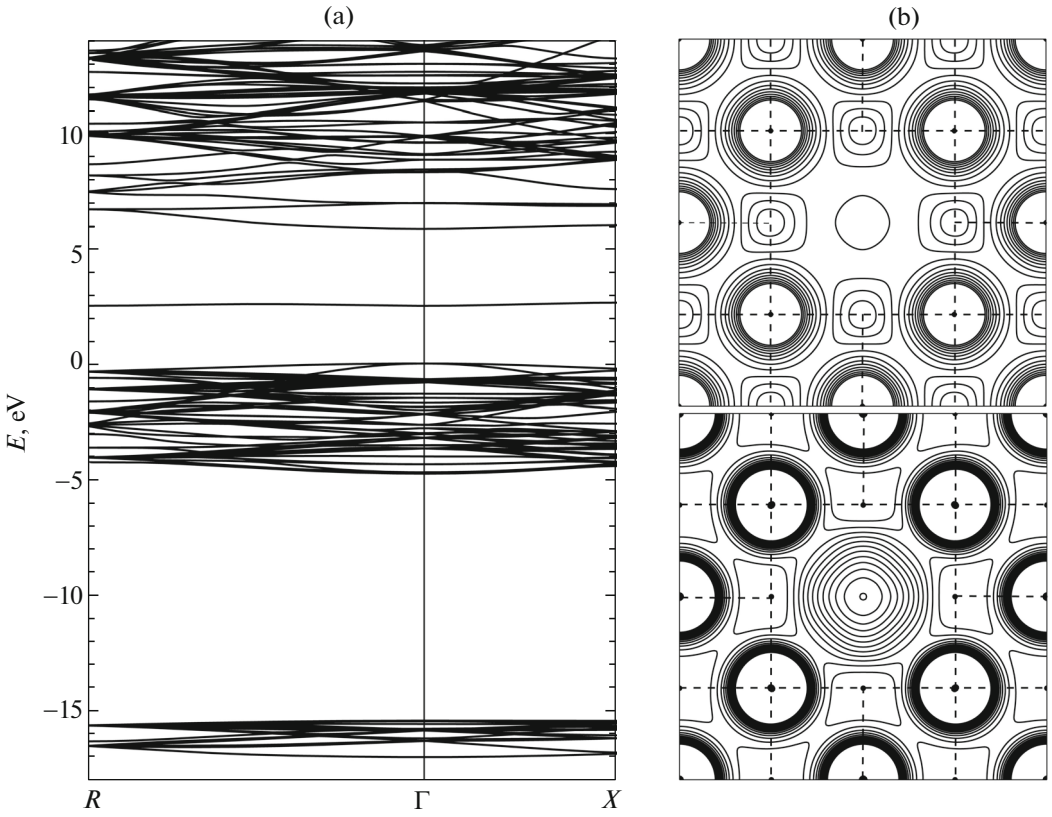

Fig. 3. (a) Band structure of MgO[F^0] and (b) electronic density: the full valence one (at the top) and the partial one from *s*-bands of oxygen and F^0-center (at the bottom).

ever, can be revealed, which is in the emergence of the satellite bands in the center of gravity of the *d*-bands in copper. As was previously observed, these states can be attributed to the change in the *p*–*d* interactions, when varying the Cl atom content in the anionic sublattice.

Figure 3a depicts the band structure of MgO with neutral oxygen vacancy defect (F^0), where the origin of the energy scale is superposed with the top of the *p*-band of the oxygen atoms for ease of analysis and further comparison with unperturbed crystal. The valence band contains 125 subbands, among which 124 correspond to *s*- and *p*-bands of oxygen and exhibit the complex miniband behavior that is induced by the effect of the multiple band folding of the perfect crystal. The main feature is the defect band of F^0-center with an energy of 2.5 eV relative to the top of the valence band, and it is characterized by vanishing dispersion, which means an isolated and strongly localized behavior of the electronic states. The results of the calculations are in good agreement with the recent calculations in the localized basis [26].

The energy bands of the perfect crystal with a 64-atom cell and of the appropriate defect crystal with the unit oxygen vacancy, unfolded in the Brillouin zone of a face-centered PC-lattice, are shown in Fig. 4. As is seen, the greatest weight of the F^0-center band is observed at the Γ point that proves the above conclusion. The main advantage of the unfolding method is in the capability it allows to monitor the changes in the electronic structure of the perfect crystal, caused by perturbation. For system MgO[F^0] (Fig. 4b), it is obvious that the lowest *s*-band is completely recovered at the unfolding, exhibiting no visual ruptures or shifts, which indicates the absence of the considerable perturbations of the electronic states in this energy range. This feature can also be explained by the charge density distribution in the vicinity of the oxygen vacancy, which is subjected to a quasi-spherical shape (Fig. 3b), although being diffusive in comparison with the *s*-electron charge distribution of the neighboring oxygen atoms.

It is worth mentioning that the lattice strains in the vicinity of the F^0 defect are quite minor. Indeed, in accordance with the optimization results, the shifts of the nearest magnesium atoms from the vacancy center are within 0.6% of the anion–cation bond length in the defect-free MgO. The comparatively small violation of the crystal structure explains the reproduction of the characteristics of the low valence band in MgO, which is formed by the deeply lying O 2*s*-character. The more pronounced changes are observed for the

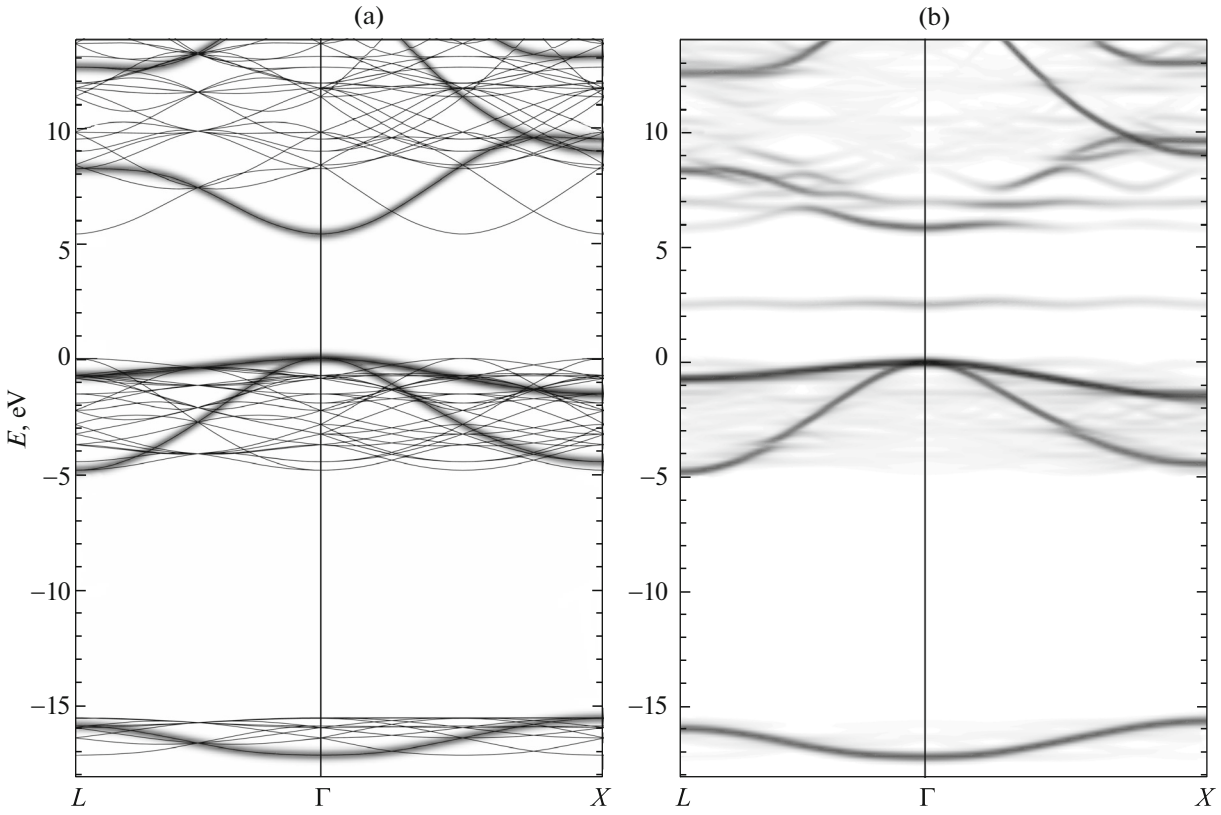

Fig. 4. Spectral function of (a) MgO perfect crystal and (b) MgO[F^0].

upper valence bands with the O 2*p*-feature. The ruptures of bands, as well as their blurs, are over the energy range from −5 to 0 eV (Fig. 4b) due to the change in the interaction behavior in the MgO oxygen sub-system. Finally, the spectrum in the conductivity band is in fact the superposition of the states of perfect crystal and of the discrete spectrum of the free F^0 center states, which modify the band structure of the perfect crystal in the range of 5 to 10 eV.

5. CONCLUSIONS

In this work we obtained the band structure unfolding formula that combines the advantages of the basis of the localized functions and plane waves, unlike the previously proposed analogues. The validity of the expression was demonstrated by an example of a perfect silicon lattice for different four- and eight-fold expansions of the unit cell. The application of the band unfolding method for copper halide alloys and for MgO crystal with a vacancy defect enabled us to analyze the changes in the energy spectra of the considered compounds and to reveal the features which are not seen when studying electronic states of the systems with complex composition and structure via the standard methods.

ACKNOWLEDGMENTS

This study was supported by the Tomsk State University Academic D.I. Mendeleev Fund Program (project no. 8.2.10.2015) and the Ministry of Education and Science of the Russian Federation (project no. 3.1235.2014K).

REFERENCES

1. R. A. Evarestov, *Quantum-Chemical Methods in Solid State Theory* (Leningrad State University, Leningrad, 1982) [in Russian].
2. T. G. Dagram, R. B. Capaz, and B. Koiler, Phys. Rev. B: Condens. Matter **56**, 9625 (1997).
3. L.-W. Wang, L. Bellaiche, S.-H. Wei, and A. Zunger, Phys. Rev. Lett. **80**, 4725 (1998).
4. T. B. Boykin and G. Klimeck, Phys. Rev. B: Condens. Matter **71**, 115215 (2005).
5. T. B. Boykin, N. Kharche, G. Klimeck, and M. Korkusinski, J. Phys.: Condens. Matter **19**, 036203 (2007).
6. T. Boykin, N. Kharche, and G. Klimeck, Phys. Rev. B: Condens. Matter **76**, 035310 (2007).
7. W. Ku, T. Berlijn, and C.-C. Lee, Phys. Rev. Lett. **104**, 216401 (2010).
8. V. Popescu and A. Zunger, Phys. Rev. B: Condens. Matter **85**, 085201 (2012).

9. M. Tomic, H. O. Jeschke, and R. Valenti, Phys. Rev. B: Condens. Matter **90**, 195121 (2014).
10. O. Rubel, A. Bokhanchuk, S. J. Ahmed, and E. Assmann, Phys. Rev. B: Condens. Matter **90**, 115202 (2014).
11. C.-C. Lee, Y. Yamada-Takamura, and T. Ozaki, J. Phys.: Condens Matter **25**, 345501 (2013).
12. P. B. Allen, T. Berlijn, D. A. Casavant, and J. M. Soler, Phys. Rev. B: Condens. Matter **87**, 085322 (2013).
13. H. Huang, F. Zheng, P. Zhang, J. Wu, B.-L. Gu, and W. Duan, New J. Phys. **16**, 033034 (2014).
14. M. Farjam, J. Phys.: Condens Matter **26**, 155502 (2014).
15. P. V. C. Medeiros, S. Stafström, and J. Björk, Phys. Rev. B: Condens. Matter **89**, 041407 (2014).
16. R. W. Jansen and O. F. Sankey, Phys. Rev. B: Condens. Matter **36**, 6520 (1987).
17. A. B. Gordienko and A. S. Poplavnoi, Russ. Phys. J. **40** (1), 47 (1997).
18. A. B. Gordienko and A. S. Poplavnoi, Phys. Status Solidi B **202**, 941 (1997).
19. A. Ceperley and B. Alder, Phys. Rev. Lett. **45**, 566 (1980).
20. J. P. Perdew and A. Zunger, Phys. Rev. B: Condens. Matter **23**, 5048 (1981).
21. H. J. Monkhorst and J. D. Pack, Phys. Rev. B: Solid State **13**, 5188 (1976).
22. C. Hartwigsen, S. Goedecker, and J. Hutter, Phys. Rev. B: Condens. Matter **58**, 3641 (1998).
23. A. V. Kosobutsky and A. B. Gordienko, Phys. Solid State **57** (10), 1972 (2015).
24. F. O. Lucas, A. Mitra, P. J. McNally, S. Daniels, A. L. Bradley, D. M. Taylor, Y. Y. Proskuryakov, K. Durose, and D. C. Cameron, J. Phys. D: Appl. Phys. **40**, 3461 (2007).
25. K. V. Rajani, S. Daniels, M. Rahman, A. Cowley, and P. J. McNally, Mater. Lett. **111**, 63 (2013).
26. E. Ertekin, L.K. Wagner, and J. C. Grossman, Phys. Rev. B: Condens. Matter **87**, 155210 (2013).

Translated by O. Maslova